

HDAC6/FOXP3/HNF4 α Axis Promotes Bile Acids Induced Gastric Intestinal Metaplasia

Na Wang

Fourth Military Medical University: Air Force Medical University

Siran Wu

Fourth Military Medical University: Air Force Medical University

Luyao Zhang

Fourth Military Medical University: Air Force Medical University

Min Chen

Fourth Military Medical University: Air Force Medical University

Jiaoxia Zeng

Fourth Military Medical University: Air Force Medical University

Guofang Lu

Fourth Military Medical University: Air Force Medical University

Fenli Zhou

Fourth Military Medical University: Air Force Medical University

Qiong Wu

Fourth Military Medical University: Air Force Medical University

Junye Liu

Fourth Military Medical University: Air Force Medical University

Yongquan Shi (✉ shiyquan@fmmu.edu.cn)

Fourth Military Medical University <https://orcid.org/0000-0001-9515-7577>

Primary research

Keywords: Gastric intestinal metaplasia, HDAC6, FOXP3, HNF4 α , Gastric cancer

Posted Date: January 29th, 2021

DOI: <https://doi.org/10.21203/rs.3.rs-155411/v1>

License:   This work is licensed under a Creative Commons Attribution 4.0 International License.

[Read Full License](#)

Abstract

Background: Gastric intestinal metaplasia (IM) is an important precancerous lesion. Our previous study has shown that ectopic expression of HDAC6 promotes the activation of intestinal markers in bile acids (BA) induced gastric IM cells; however, the mechanism underlying how HDAC6-mediated epigenetic modifications regulate intestinal markers is not clear.

Methods: RNA-sequencing (RNA-seq) was used to detect the molecular changes in GES-1 cells after HDAC6 overexpression. The potential binding sites of FOXP3 with the promoter region of HNF4 α were verified by ChIP and luciferase reporter gene assays. The ChIP assay was also used to detect the histone deacetylation. The levels of mucin in gastric or intestinal mucosa were detected by AB-PAS staining. Transgenic mice were used to explore the pro-metaplastic function of DCA and HNF4 α in vivo.

Results: Deoxycholic acid (DCA) upregulated HDAC6 in gastric cells, which further inhibited the transcription of FOXP3. Then, FOXP3 transcriptionally inhibited HNF4 α , which further inhibits the expression of downstream intestinal markers. These molecules have been shown to be clinically relevant, as FOXP3 levels were negatively correlated with HDAC6 and HNF4 α in IM tissues. Transgenic mice experiments confirmed that HNF4 α overexpression combined with DCA induced gastric mucosa to secrete intestinal mucus and caused an abnormal mucosal structure.

Conclusions: Our findings suggest that HDAC6 reduces FOXP3 through epigenetic modification, thus forming HDAC6/FOXP3/HNF4 α axis to promote gastric IM. Inhibition of HDAC6 may be a potential approach to prevent gastric IM in patients with bile reflux.

Background

Gastric cancer (GC) is the third most common cause of cancer-related death in the worldwide [1]. According to the Lauren classification, GC mainly includes the intestinal type and the diffused type. Intestinal-type GC follows the Correa development model, namely, chronic superficial gastritis, atrophic gastritis, intestinal metaplasia (IM), dysplasia, and finally to GC [2].

Gastric IM refers to the replacement of gastric mucosa cells by intestinal-type cells. This process is thought to be caused by chronic environmental stimulation, among which *Helicobacter pylori* (*Hp*) is considered to be the main cause of IM [3-5]; however, it is worth noting that some studies have shown that eradication of *Hp* cannot completely stop the progression of IM to GC [6, 7]. This fact suggests that in addition to *Hp*, other factors, such as bile reflux, may play an important role in promoting the occurrence and malignant progression of IM [8-10]. In recent years, many in vivo and in vitro studies on Barrett's esophagus (BE) have confirmed that bile acids (BA) promote esophageal mucosa IM [11-13].

In a previous study, we successfully constructed a BA-induced IM cell model, in which Caudal-related homeobox transcription factor 2 (CDX2) and other intestinal markers were significantly increased [14]. In addition, we found that HNF4 α , an important transcription factor (TF) involved in the differentiation and

development of the liver and intestine [15-17], forms a closed loop by interacting with HDAC6, and promotes the continuous progression of IM under the regulation of miR-1 [18]. In this loop, HNF4 α can activate HDAC6 promoter, but how HDAC6 regulates HNF4 α remains unclear. Epigenetic modification is considered to be an important mechanism driving the development of GC [19-21]. In particular, histone acetyltransferase (HATs) and histone deacetylase (HDACs) can modify the lysine residues of histone or nonhistone after translation, and their balance promotes the maintenance of cell homeostasis [22-24]. The abnormal expression of HDAC6 is reportedly involved in the occurrence and development of various human cancers [25-27]; however, the role of epigenetic modification mediated by HDACs in the progression of GC or IM remains unclear. To identify the downstream target of HDAC6, we conducted RNA-sequencing (RNA-seq) and bioinformatics analyses. The results showed that FOXP3, which has potential binding sites for the HNF4 α promoter, might be the modified target of HDAC6. Therefore, we hypothesize that HDAC6 may regulate HNF4 α transcription through histone deacetylation of FOXP3, and eventually form a complete HDAC6/FOXP3/HNF4 α loop.

FOXP3 is an essential TF that maintain the immunosuppressive function of regulatory T cells (Tregs) and plays an important role in maintaining immune homeostasis [28-30]. FOXP3 can also be expressed in tissue cells [31, 32]. For example, in breast cancer cells, FOXP3 promotes the expression of SKP2 and stimulates the cell proliferation [33]; in non-small cell lung cancer (NSCLC), FOXP3 enhances tumor growth by activating the WNT/ β -Catenin pathway via Gli1 activation [34]; FOXP3-c-MYC signaling regulates tumor progression in prostate cancer [35]. However, no consensus has been reaching regarding the role of FOXP3 in GC. Some studies have shown that FOXP3 can promote tumor occurrence in gastric cells, while other studies have revealed that it may inhibit the progression of GC [36, 37]. Furthermore, the role of FOXP3 in IM has not yet been reported.

In this study, we found that HDAC6 triggered the deacetylation of the *FOXP3* locus to inhibit its transcription during BA-induced gastric IM. Decrease of FOXP3 stimulated the transcription of HNF4 α . Finally, HDAC6, FOXP3 and HNF4 α formed a closed loop to promote the progression of gastric IM under BA stimulation. Blocking of this circuit may prevent BA-induced IM and even GC.

Methods

Cell lines

The cell model of BA-induced gastric IM was constructed as previously reported [14]. To imitate the situation of bile reflux in gastric mucosa as much as possible, we used the immortalized gastric mucosa cell line GES-1 cells and primary mouse gastric mucosa cells to carry out the BA stimulation experiment. GES-1 and AGS cells (originally purchased from ATCC) were cultured in 1640 medium (Gibco, USA) with 10% fetal bovine serum (Biological Industries, Israel). Deoxycholic acid (DCA) a kind of bile acid with strong cytotoxicity, was purchased from Biocytosci (USA).

Animals

We previously constructed transgenic mice with Lgr5+ gastric mucosal stem cells specifically expressing Hnf4a [18]. In this study, sixteen *WT* mice and sixteen tamoxifen activated transgenic mice *ROSA26^{Hnf4a}* aged 3 months were randomly divided into two groups: one group was treated with deoxycholic acid (DCA) while the control group was treated with PBS. The mice in the DCA group were given BA (0.3% DCA, pH 7.0) in the drinking water for 12 months, and PBS was added to the control group. The dose was determined according to the article of Quante et al [11]. Tamoxifen was given 6 weeks before BA treatment. All animal experiments were approved by Animal Research Committee of Xijing Hospital.

Tissue

An IM tissue microarray including 80 cases (#ST8017a) and a gastritis tissue microarray including 24 cases (#Sto01007) were purchased from Alenabio Company (China). Ten pairs of matched IM and para metaplasia tissues were taken from the Endoscopy Center of Xijing Hospital of Digestive Diseases and diagnosed as gastric IM by the Department of Pathology. The collected tissues were immediately frozen into liquid nitrogen for preservation. To exclude the influence of *Hp*, the selected tissues were all negative for *Hp*. Before the specimens were obtained, all patients signed the informed consent. This study was approved by the Human Subjects Committee of Xijing Hospital.

RNA-sequencing

GES-1 cells were infected with HDAC6 overexpression virus vector or negative control virus vector, and then treated with puromycin to establish stable cell line. Total RNA was extracted using RNeasy Micro Kit (Cat# 74004, Qiagen, Germany) following the manufacturer's instructions and checked for a RIN number to inspect RNA integrity by an Agilent Bioanalyzer 2100 (Agilent technologies, Santa Clara, USA). Qualified total RNA was further purified by RNAClean XP Kit (Cat A63987, Beckman Coulter, Inc. Kraemer Boulevard Brea, USA) and RNase-Free DNase Set (Cat#79254, Qiagen, Germany). Edger was used to analyze the differentially expressed genes among samples. After obtaining the p-value, multiple hypothesis tests were conducted. The threshold value of p-value was determined by controlling FDR (false discovery rate). The corrected p-value is q-value. At the same time, we calculated the differential expression multiple (fold change) according to the FPKM value.

Transfection and infection

HDAC6, FOXP3, HNF4a and EP300 overexpression lentiviral vectors were purchased from Genechem Co. Ltd. (China). The small interference RNAs (siRNAs) to HDAC6, FOXP3 and HNF4a were purchased from Genepharma (China). Three pairs of primer sequences were designed for each gene, and the one with the highest knockdown efficiency was used in this study. The sequences are shown in Table 1. The transfection reagent was used following the manufacturer's protocol (Thermo Fisher Scientific, USA).

Quantitative real-time PCR

Cellular RNA was extracted using TRIzol® reagent (Invitrogen, USA) according to the standard protocol. Then RNA reverse transcribed into cDNA using the Evo M-MLV RT Kit, and qPCR was performed using the SYBR Green Premix Pro Taq HS qPCR Kit (Accurate Biotechnology (Hunan) Co., Ltd, China) on a CFX96™ Real-Time PCR Detection system (Bio-Rad Laboratories, USA). The $2^{-\Delta\Delta Cq}$ method was used to calculate the relative mRNA expression of each gene with β -actin as the internal control. The primer sequences of each gene are provided in Table 2.

Immunoblot analysis

Immunoblot analysis was conducted using standard procedures. The following antibodies were used in this study: anti-HDAC6 (1:1000, Cell Signaling Technology, #7558), anti-FOXP3 (1:2000, abcam, #ab10901), anti-HNF4 α (1:2000, abcam, #ab72378), anti-CDX2 (1:1000, Cell Signaling Technology, #12306), anti-KLF4 (1:1000, Cell Signaling Technology, #12173), anti-MUC2 (1:4000, abcam, ab134119) and anti- β -actin (1:5000, Bioworld, #AP0060). Target molecule expression was detected by the chemiluminescence method.

Immunohistochemistry and AB-PAS staining

Paraffin-embedded sections were deparaffinized and antigens were repaired. Slides were preblocked and then incubated with primary antibodies at 4°C overnight. The slides were incubated with anti-rabbit antibodies for 40 minutes and stained with DAB substrate. Nuclei were stained using hematoxylin. The following primary antibodies were used: anti-FOXP3 (1:1000, abcam, #ab10901), anti-HDAC6 (1:400, Cell Signaling Technology, #7558) and anti-HNF4 α (1:300, abcam, #ab72378). CDX2 staining in IM tissues was used as positive control and PBS as negative control. The immunohistochemistry (IHC) staining score was calculated as previously described¹⁴. The IHC staining results were evaluated by two pathologists independently. Alcian blue staining-periodic acid-Schiff (AB-PAS) staining was performed according to the manufacturer's protocol (Solarbio, China).

Immunofluorescence

Immunofluorescence (IF) staining for FOXP3 was conducted in GES-1 cells. The cells were plated in 4-well chamber slides (Millipore, USA), washed with PBS and fixed with 4% paraformaldehyde for 30 minutes. Next, the cells were permeabilized with Triton X-100 for 10 minutes and blocked with sheep serum for 30 minutes. The cells were then incubated with FOXP3 primary antibody (1:200, abcam, #ab10901) overnight at 4°C in a humidified chamber followed by incubation with a FITC secondary antibody (1:200, EMD Millipore, #3051741) for 2 hours at room temperature in the dark. The nuclei were stained with DAPI (1:800, Solarbio, #c0060). The slides were examined using a Fluoview FV1200 Laser Scanning Confocal Microscope (Olympus Corp.).

Luciferase reporter assays

The luciferase reporter assay was conducted as previously described [18]. The promoter sequence of HNF4 α was as follow: 5'-cgacgcgtAAAATATTAATACTTTTTTTTTTTCTGAGATG-3'. PGL3 basic was used as the negative control.

Chromatin immunoprecipitation assay

Chromatin immunoprecipitation (ChIP) assay was also conducted as previously described¹⁸. HDAC6 (ActiveMotif, #40971), H3ac (ActiveMotif, #39040), H4ac (ActiveMotif, #39026), H3K9 (abcam, #ab32129), H3K27 (abcam, #ab177178) and FOXP3 antibodies (abcam, #ab10901) were used to precipitate DNA that used for PCR amplification of their binding sites in FOXP3 or HNF4 α genes. The sequences were shown in Table 2.

Statistical analysis

SPSS software (v.19.0, SPSS, Chicago, Illinois, USA) was used for statistical analysis. The continuous data between two groups were compared by Student's unpaired t-test, and the results are presented as the mean \pm SEM. Frequencies of categorical variables were compared using the χ^2 test. $P < 0.05$ was considered statistically significant (* $P < 0.05$, ** $P < 0.01$).

Results

Predicted downstream targets of HDAC6

To explore the role of HDAC6 mediated epigenetic modification in BA-induced gastric IM, we transfected GES-1 cells with HDAC6 overexpression or negative control viruses and then performed RNA-seq. From the heat map, we could see that the overexpression of HDAC6 can reduce the expression of various genes in GES-1 cells (Fig. 1a). KEEG data showed that abnormally expressed genes induced by HDAC6 were mainly involved in the signaling pathways related to tumor or signal transduction (Fig. 1b). Considering that the deacetylation of HDACs on the histone of the target gene can inhibit its transcription, we crossed the downregulated genes after HDAC6 overexpression with the genes after DCA treatment in GES-1 cells [18] (Fig. 1c). STOX1, BLOC1S5-TXNDC5 and FOXP3 were identified (Fig. 1d). Through bioinformatics analysis, we found that FOXP3 has potential binding sites in the promoter region of HNF4 α . Therefore, we hypothesized that FOXP3 may be an HDAC6 target that connects to HNF4 α .

HDAC6 and DCA decreased FOXP3 in gastric cells

We first assessed the effect of DCA on FOXP3 expression. The results showed that compared with the control group, DCA significantly reduced FOXP3 expression at both mRNA level and protein level in GES-1 cells and mouse primary gastric mucosa cells (Fig. 2a, 2b). The immunofluorescence results showed that DCA inhibited FOXP3 in GES-1 cells (Fig. 2c). We also found that, after HDAC6 overexpression in GES-1 cells, the FOXP3 protein and mRNA levels decreased significantly (Fig. 2d, 2e). In contrast, FOXP3 was

significantly increased in AGS cells after HDAC6 knockdown compared with control cells (Fig. 2f, 2g). Together, these results suggest that DCA and HDAC6 can induce decreased FOXP3 levels in gastric cells.

FOXP3 is decreased in IM tissues and negatively correlated with HDAC6 and HNF4α

To investigate the relevance of FOXP3 with gastric IM clinically, we examined its expression in IM and gastritis tissues. The results showed that FOXP3 expression in IM tissues was significantly lower than in gastritis tissues (IM: 1.04 ± 2.21 , gastritis: 2.68 ± 3.20 , $p=0.0049$), and was located in the nucleus and cytoplasm (Fig. 3a, 3b). Then, we analyzed the correlation between FOXP3, HDAC6 and HNF4α in IM tissues. Both HDAC6 and HNF4α were negatively correlated with FOXP3 (Fig. 3c, 3d, Table 3). In addition, the mRNA level was lower in IM tissues than in surrounding tissues (Fig. 3e). The correlation analyses were consistent with the immunohistochemistry staining results (Fig. 3f). These results indicate that FOXP3 is decreased in IM tissues and negatively correlated with HDAC6 and HNF4α.

FOXP3 mediates the regulation of HDAC6 on intestinal markers

To further explore the regulatory effect of FOXP3 on intestinal markers, we assessed the expression changes of downstream molecules after altering the expression levels of HDAC6 and FOXP3 in gastric cells. The results showed that, after transfection with siFOXP3 in GES-1 cells, decrease of FOXP3 was accompanied by a significant increase of these markers (Fig. 4a); however, upon FOXP3 overexpression in AGS cells, the intestinal markers decreased significantly compared with the control group (Fig. 4b). We then infected GES-1 cells with an HDAC6 overexpression vector and FOXP3 overexpression vector simultaneously. The promotion effect of HDAC6 on HNF4α and downstream intestinal markers was partially reversed by FOXP3 (Fig. 4c). Conversely, in AGS cells treated with siHDAC6, the decrease in the downstream markers was increased by siFOXP3 (Fig. 4d). Collectively, these results indicate that FOXP3 can negatively regulate downstream intestinal markers and mediates their regulation by HDAC6.

HDAC6 promotes histone deacetylation at the *FOXP3* loci

It is well known that HATs can open gene locus and promote its transcription. On the contrary, HDACs induces gene locus closure and inhibits its transcription (Fig. 5a). To clarify how HDAC6 regulates FOXP3, we examined the epigenetic changes at the *FOXP3* loci. The sequences of the FOXP3 promoter and CNS region were shown in Figure 5b. First, the acetylation level of histone H3Ac, H3K9Ac, H3K27Ac and H4Ac in the *FOXP3* locus was detected after DCA treatment or HDAC6 overexpression in GES-1 cells. The acetylation level of them in the DCA groups was significantly lower compared to their control groups respectively (Fig. 5c). Then, the ChIP assays were performed to verify that HDAC6 could directly bind to the FOXP3 promoter (Fig. 5d). Moreover, we could see that histone acetyltransferase EP300 overexpression promoted FOXP3 expression and inhibited HNF4α (Fig. 5e), which further indicated that the FOXP3 expression level in gastric cells was regulated by histone acetylation modification. Collectively, these results indicate the importance of epigenetic regulation in DCA or HDAC6 induced suppression of FOXP3.

FOXP3 inhibits HNF4a transcription

Then, to clarify the relationship between FOXP3 and HNF4a, we examined the effect of FOXP3 on HNF4a expression. First, FOXP3 was overexpressed or knocked down in AGS and GES-1 cells respectively. The immunoblot and qRT-PCR results showed that FOXP3 negatively regulated HNF4a in gastric cells (Fig. 6a). Next, the luciferase reporter assays showed that DCA or siFOXP3 treatment promoted the HNF4a promoter activity (Fig. 6b). ChIP assay further indicated that FOXP3 could bind to the ChIP 2 and ChIP 3 sequences of the HNF4a promoter, and DCA promoted the combination (Fig. 6c). In addition, we examined the regulatory effect of FOXP3 on downstream intestinal markers mediated by HNF4a. Decreased levels of MUC2, KLF4 and CDX2 induced by FOXP3 overexpression in AGS cells was reversed by HNF4a overexpression (Fig. 6d); however, the simultaneous transfection of GES-1 cells with siFOXP3 and siHNF4a resulted in decreased activation of downstream intestinal markers (Fig. 6e). Together, these results suggest that FOXP3 can inhibit the transcription of HNF4a, and HNF4a can mediate the regulation of FOXP3 on intestinal markers.

DCA promotes intestinal mucus secretion in Hnf4a transgenic mice

To verify the effect of DCA on gastric mucosa and the expression level of Foxp3 in gastric mucosa in vivo, we treated the Hnf4a transgenic mouse model with DCA (Fig. 7a). As shown in Figure S1a [Additional file 1](#), after 12 months of DCA treatment, compared with the *Ctrl// WT* and *DCA// WT* mice, we observed significantly enlarged abnormal glands near the squamous epithelium at the squamocolumnar junction (SCJ) of *Ctrl// Rosa26^{Hnf4a}* mice and *DCA// Rosa26^{Hnf4a}* mice, which were more serious in the DCA treated transgenic mice. Further, gastric mucosal atrophy was observed in the *Ctrl// Rosa26^{Hnf4a}* mice and *DCA// Rosa26^{Hnf4a}* mice. The number of mice with different gastric mucosal lesions in each group was shown in Table 4. Then, we collected the small intestine and large intestine tissues of the *Ctrl// WT* mice for AB-PAS staining. The gastric mucosa of the other three groups showed light purple staining, while the *DCA// Rosa26^{Hnf4a}* mice showed the same staining as goblet cells in the intestinal tissue, indicating that intestinal mucus secretion may occur ([Additional file 1: Figure S1b](#)) (data of other two groups not shown). The AB-PAS staining results also showed obvious blue staining in the *Ctrl// Rosa26^{Hnf4a}* mice and *DCA// Rosa26^{Hnf4a}* mice, with the strongest staining was found in the latter group ([Additional file 1: Figure S1c](#)). The expression levels of Hdac6, Foxp3 and Hnf4a in these tissues were also detected. The Foxp3 levels in the *Ctrl// WT* and *DCA// WT* mice were significantly higher compared to the *Ctrl// Rosa26^{Hnf4a}* mice, and DCA treatment further reduced Foxp3 expression. In contrast, the expression of Hnf4a was enhanced in the *Ctrl// Rosa26^{Hnf4a}* mice coinciding with increased Hdac6. DCA treatment further induced the expression of Hnf4a and Hdac6 in the transgenic mice (Fig. 7b, 7c). Collectively, these findings indicate that Hnf4a transgenic mice undergo gastric mucosal changes in the SCJ region similar to BE and atrophy in gastric antrum. Moreover, Hnf4a promotes Hdac6 but inhibits Foxp3, which is consistent with the results of the in vitro experiments.

Conclusion

In this study, we confirmed the important role of HDAC6 mediated epigenetic modification in BA-induced gastric IM. HDAC6 causes chromatin remodeling at the *FOXP3* locus under DCA treatment which induces downregulation of *FOXP3* in gastric cells. Reduced levels of *FOXP3* enhances the transcription of *HNF4a*. Therefore, HDAC6/*FOXP3*/*HNF4a* axis promotes BA-induced gastric IM and may be involved in the development of GC.

HDAC6, which is classified in class II HDACs, could close DNA to inhibit transcription. HDAC6 is reportedly involved in tumor progression, such as oral cancer and leukemia [38-39]. Similarly, HDAC6 was overexpressed in GC cells, and inhibition of HDAC6 could significantly reduce cell proliferation [40]. Activation of the Akt/TYMS signaling pathway mediated by HDAC6 also participates in apoptosis and chemoresistance of GC cells [41]. In a previous study, we found that HDAC6 and *HNF4a* formed a loop to promote gastric IM under the regulation of miR-1 [18]. *HNF4a*, as a transcription factor, stimulates HDAC6 transcription; however, how HDAC6 activates *HNF4a* or promotes IM remains unclear. HDAC6 inhibitors can promote *FOXP3* expression by regulating acetylation of the gene, thus promoting the immunosuppressive effect of Treg cells [42]. At the same time, bioinformatics analysis found that *FOXP3* has putative binding sites for the *HNF4a* promoter, so we hypothesized that *FOXP3* might be the downstream modification target of HDAC6. We first provided evidence that HDAC6 overexpression and BA could decrease the mRNA and protein levels of *FOXP3*. In addition, *FOXP3* negatively regulated *MUC2*, *KLF4* and *CDX2* which suggested that this molecule may be involved in BA-induced IM.

Recently, the role of *FOXP3* in tumor development, in a Treg independent manner, has attracted increasing attention. Most studies have shown that this molecule is associated with poor prognosis of cancer patients [43, 44]. Both in vivo and in vitro studies have confirmed that *FOXP3* plays an anti-cancer role in breast cancer and prostate cancer. In this study, we found that the expression of *FOXP3* in gastritis tissues was significantly higher than in IM tissues. In vitro experiments further confirmed that *FOXP3* could be involved in the regulation of HDAC6 on downstream *HNF4a* and intestinal markers. To determine whether HDAC6 regulated *FOXP3* by epigenetic modification, we analyzed the histone acetylation level at *FOXP3* locus after DCA treatment, and H3Ac, H3K9Ac, H3K27Ac and H4Ac showed significant suppression. Furthermore, ChIP assays confirmed that HDAC6 could directly bind to the *FOXP3* promoter. The results also showed that *FOXP3* can inhibit the transcription of *HNF4a*, which subsequently affects the downstream intestinal markers. The above results of this study combined with previous studies showed that miR-1 decreased under the stimulation of BA, leading to increased expression of downstream target molecules *HNF4a* and HDAC6, and *HNF4a* further increased HDAC6 promoter activity. Additionally, HDAC6 reduced *FOXP3* through epigenetic modification which could further increase *HNF4a* through transcriptional suppression, thus forming a closed loop that promotes the activation of intestinal markers and IM occurrence.

Another important finding of this study is that DCA treatment of *Hnf4a* transgenic mice for 12 months caused gastric mucosa atrophy at the antrum and abnormal columnar glands at the SCJ of gastric mucosa which is similar to the histopathologic changes in L2-IL-1 β mice reported by Quante et al [45]. Compared with *Ctrl/Rosa26^{Hnf4a}* mice, gastric mucosa inflammation and intestinal mucus secretion were

more obvious in the *DCA/Rosa26^{Hnf4a}* mice. Furthermore, the Hdac6, Hnf4α and Foxp3 expression levels in the gastric mucosal cells before and after BA stimulation was examined, and the results were consistent with the in vitro results and further indicated the existence of HDAC6/FOXP3/HNF4α regulatory loop. Unfortunately, we did not detect the expression of intestinal markers TFF3 and MUC2 in mouse gastric mucosa containing goblet like cells (data not shown). We will continue to review the literature to find more suitable molecules and examine them in these tissues. In addition, it is noteworthy that the establishment of a bile reflux mouse model in the future may better verify our hypothesis.

In conclusion, this study demonstrated that HDAC6 stimulated by BA could epigenetically regulate FOXP3, which promoted gastric IM by inhibiting HNF4α transcription. Therefore, we propose a model of BA-induced gastric IM (Fig. 6f). The activation of the HDAC6/FOXP3/HNF4α loop regulated by miR-1 promotes BA-induced gastric IM. The inhibition of HDAC6 may break this loop and prevent the occurrence of gastric IM or even GC in patients with bile reflux.

Abbreviations

GC: gastric cancer; IM: intestinal metaplasia; BA: bile acids; DCA: Deoxycholic acid; *Hp*: *Helicobacter pylori*; CDX2: homeobox transcription factor 2; TF: transcription factor; HATs: histone acetyltransferase; HDACs: histone deacetylase; RNA-seq: RNA-sequencing; siRNAs: small interference RNAs; ChIP: Chromatin immunoprecipitation.

Declarations

Ethics approval and consent to participate

All patients signed the informed consent before the specimens were obtained. This part of study was approved by the Human Subjects Committee of Xijing Hospital. All animal experiments were approved by Animal Research Committee of Xijing Hospital.

Consent for publication

All authors have agreed to publish this manuscript.

Availability of data and materials

All data generated during this study are included in this article.

Competing interests

The authors declare no potential conflicts of interest.

Funding

This work was supported by grant from National Natural Science Foundation of China (No. 81873554 to YQS). This study was supported in part by Shaanxi Innovation Promotion Project (NO. 2018TD-003 to YQS) and independent project of State Key Laboratory of cancer biology (NO. CBSKL2019ZZ07 to YQS).

Author contributions

All authors included in this paper fulfill the criteria of authorship and have approved the submission of this manuscript. NW, JYL and YQS designed the experiments. NW, SRW, LYZ, MC, JXZ, GFL, FLZ and QW performed the study. JYL and YQS supervised the study. All authors read and approved the final manuscript.

Acknowledgements

We wish to thank Zhang Lifeng and Yong Guo (Xijing Hospital of Digestive Diseases) for technical assistance.

References

1. Bray F, Ferlay J, Soerjomataram I, Siegel RL, Torre LA, Jemal A. Global cancer statistics 2018: GLOBOCAN estimates of incidence and mortality worldwide for 36 cancers in 185 countries. *CA Cancer J Clin.* 2018;68:394-424.
2. Correa P. Human gastric carcinogenesis: a multistep and multifactorial process—First American Cancer Society Award Lecture on Cancer Epidemiology and Prevention. *Cancer Res.* 1992;52:6735-40.
3. Chuang CH, Yang HB, Sheu SM, Hung KH, Wu JJ & Cheng HC, et al. Helicobacter pylori with stronger intensity of CagA phosphorylation lead to an increased risk of gastric intestinal metaplasia and cancer. *BMC Microbiol.* 2011;11:121.
4. Sue S, Shibata W & Maeda S. Helicobacter pylori-Induced Signaling Pathways Contribute to Intestinal Metaplasia and Gastric Carcinogenesis. *Biomed Res Int.* 2015;2015:737621.
5. Saikawa Y, Fukuda K, Takahashi T, Nakamura R, Takeuchi H & Kitagawa Y. Gastric carcinogenesis and the cancer stem cell hypothesis. *Gastric Cancer* 2010;13:11-24.
6. Leung WK, Lin SR, Ching JY, To KF, Ng EK, Chan FK, et al. Factors predicting progression of gastric intestinal metaplasia: results of a randomised trial on Helicobacter pylori eradication. *Gut.* 2004;53:1244-9.
7. Lee YC, Chen TH, Chiu HM, Shun CT, Chiang H, Liu TY, et al. The benefit of mass eradication of Helicobacter pylori infection: a community-based study of gastric cancer prevention. *Gut.* 2013;62:676-82.
8. Jiang JX, Liu Q, Zhao B, Zhang HH, Sang HM, Djaleel SM, et al. Risk factors for intestinal metaplasia in a southeastern Chinese population: an analysis of 28,745 cases. *J Cancer Res Clin Oncol.* 2017;143:409-418.

9. Debruyne PR, Witek M, Gong L, Birbe R, Chervoneva I, Jin T, et al. Bile acids induce ectopic expression of intestinal guanylyl cyclase C Through nuclear factor-kappaB and Cdx2 in human esophageal cells. *Gastroenterology*. 2006;130:1191-206.
10. Tatsugami M, Ito M, Tanaka S, Yoshihara M, Matsui H, Haruma K, et al. Bile acid promotes intestinal metaplasia and gastric carcinogenesis. *Cancer Epidemiol Biomarkers Prev*. 2012;21:2101-7.
11. Quante M, Bhagat G, Abrams JA, Marache F, Good P, Lee MD, et al. Bile acid and inflammation activate gastric cardia stem cells in a mouse model of Barrett-like metaplasia. *Cancer Cell*. 2012;21:36-51.
12. Kazumori H, Ishihara S, Rumi MA, Kadowaki Y & Kinoshita Y. Bile acids directly augment caudal related homeobox gene Cdx2 expression in oesophageal keratinocytes in Barrett's epithelium. *Gut*. 2006;55:16-25.
13. Debruyne PR, Witek M, Gong L, Birbe R, Chervoneva I, Jin T, et al. Bile acids induce ectopic expression of intestinal guanylyl cyclase C Through nuclear factor-kappaB and Cdx2 in human esophageal cells. *Gastroenterology*. 2006;130:1191-206.
14. Li T, Guo H, Li H, Jiang Y, Zhuang K, Lei C, et al. MicroRNA-92a-1-5p increases CDX2 by targeting FOXD1 in bile acids-induced gastric intestinal metaplasia. *Gut*. 2019;68:1751-1763.
15. Chen L, Toke NH, Luo S, Vasoya RP, Fullem RL, Parthasarathy A, et al. A reinforcing HNF4-SMAD4 feed-forward module stabilizes enterocyte identity. *Nat Genet*. 2019;51:777-785.
16. Davison JM, Lickwar CR, Song L, Breton G, Crawford GE & Rawls JF. Microbiota regulate intestinal epithelial gene expression by suppressing the transcription factor Hepatocyte nuclear factor 4 alpha. *Genome Res*. 2017;27:1195-1206.
17. Wu H, Reizel T, Wang YJ, Lapiro JL, Kren BT, Schug J, et al. A negative reciprocal regulatory axis between cyclin D1 and HNF4alpha modulates cell cycle progression and metabolism in the liver. *Proc Natl Acad Sci USA*. 2020;117:17177-17186.
18. Wang N, Chen M, Ni Z, Li T, Zeng J, Lu G, et al. HDAC6/HNF4alpha loop mediated by miR-1 promotes bile acids-induced gastric intestinal metaplasia. *Gastric Cancer*. 2021;24:103-116.
19. Zhang B, Wu Q, Li B, Wang D, Wang L & Zhou YL. m(6)A regulator-mediated methylation modification patterns and tumor microenvironment infiltration characterization in gastric cancer. *Mol Cancer*. 2020;19:53.
20. Jie M, Wu Y, Gao M, Li X, Liu C, Ouyang Q, et al. CircMRPS35 suppresses gastric cancer progression via recruiting KAT7 to govern histone modification. *Mol Cancer*. 2020;19:56.
21. Qin ZY, Wang T, Su S, Shen LT, Zhu GX, Liu Q, et al. BRD4 Promotes Gastric Cancer Progression and Metastasis through Acetylation-Dependent Stabilization of Snail. *Cancer Res*. 2019;79:4869-4881.
22. Schader T, Lowe O, Reschke C, Malacarne P, Hahner F, Muller N, et al. Oxidation of HDAC4 by Nox4-derived H2O2 maintains tube formation by endothelial cells. *Redox Biol*. 2020;36:101669.
23. Bruhn C, Ajazi A, Ferrari E, Lanz MC, Batrin R, Choudhary R, et al. The Rad53(CHK1/CHK2)-Spt21(NPAT) and Tel1(ATM) axes couple glucose tolerance to histone dosage and subtelomeric silencing. *Nat Commun*. 2020;11:4154.

24. Shao LW, Peng Q, Dong M, Gao K, Li Y, Li Y, et al. Histone deacetylase HDA-1 modulates mitochondrial stress response and longevity. *Nat Commun.* 2020;11:4639.
25. Li Z, Lu X, Liu Y, Zhao J, Ma S, Yin H, et al. Gain of LINC00624 Enhances Liver Cancer Progression by Disrupting the HDAC6-TRIM28-ZNF354C Corepressor Complex. *Hepatology.* 2020 online ahead of print.
26. Bhat-Nakshatri P, Kumar B, Simpson E, Ludwig KK, Cox ML, Gao H, et al. Breast cancer cell detection and characterization from breast milk-derived cells. *Cancer Res.* 2020;80:4828-4839.
27. Park SJ, Kim JK, Bae HJ, Eun JW, Shen Q, Kim HS, et al. HDAC6 sustains growth stimulation by prolonging the activation of EGF receptor through the inhibition of rabaptin-5-mediated early endosome fusion in gastric cancer. *Cancer Lett.* 2014;354:97-106.
28. van Loosdregt J, Vercoulen Y, Guichelaar T, Gent YY, Beekman JM, van Beekum O, et al. Regulation of Treg functionality by acetylation-mediated Foxp3 protein stabilization. *Blood.* 2010;115:965-74.
29. Khumalo J, Kirstein F, Hadebe S & Brombacher F. IL-4/Ralpha signalling in CD4+CD25+FoxP3+ T regulatory cells restrain airway inflammation via limiting local tissue IL-33. *JCI Insight.* 2020;5:e136206.
30. Helmin KA, Morales-Nebreda L, Torres AM, Anekalla KR, Chen SY, Abdala-Valencia H, et al. Maintenance DNA methylation is essential for regulatory T cell development and stability of suppressive function. *J Clin Invest.* 2020;130:6571-6587.
31. Won KY, Kim HK, Kim GY, Song MJ & Lim SJ. Hippo pathway and tumoral FOXP3 expression correlate with tumor growth in squamous cell carcinoma of the lung. *Pathol Res Pract.* 2020;216:153003.
32. Qi H, Li W, Zhang J, Chen J, Peng J, Liu Y, et al. Glioma-associated oncogene homolog 1 stimulates FOXP3 to promote non-small cell lung cancer stemness. *Am J Transl Res* 12, 1839-1850 (2020).
33. Zuo T, Liu R, Zhang H, Chang X, Liu Y, Wang L, et al. FOXP3 is a novel transcriptional repressor for the breast cancer oncogene SKP2. *J Clin Invest.* 2007;117:3765-73.
34. Yang S, Liu Y, Li MY, Ng C, Yang SL, Wang S, et al. FOXP3 promotes tumor growth and metastasis by activating Wnt/beta-catenin signaling pathway and EMT in non-small cell lung cancer. *Mol Cancer.* 2017;16:124.
35. Wu L, Yi B, Wei S, Rao D, He Y, Naik G, et al. Loss of FOXP3 and TSC1 Accelerates Prostate Cancer Progression through Synergistic Transcriptional and Posttranslational Regulation of c-MYC. *Cancer Res.* 2019;79:1413-1425.
36. Wang L, Li B, Zhang L, Li Q, He Z, Zhang X, et al. miR-664a-3p functions as an oncogene by targeting Hippo pathway in the development of gastric cancer. *Cell Prolif.* 2019;52:e12567.
37. Yin H, Chu A, Liu S, Yuan Y & Gong Y. Identification of DEGs and transcription factors involved in H. pylori-associated inflammation and their relevance with gastric cancer. *PeerJ.* 2020;8:e9223.
38. Wang XC, Ma Y, Meng PS, Han JL, Yu HY & Bi LJ. miR-433 inhibits oral squamous cell carcinoma (OSCC) cell growth and metastasis by targeting HDAC6. *Oral Oncol.* 2015;51:674-82.

39. Losson H, Gajulapalli SR, Lernoux M, Lee JY, Mazumder A, Gerard D, et al. The HDAC6 inhibitor 7b induces BCR-ABL ubiquitination and downregulation and synergizes with imatinib to trigger apoptosis in chronic myeloid leukemia. *Pharmacol Res.* 2020;160:105058.
40. Park SJ, Kim JK, Bae HJ, Eun JW, Shen Q, Kim HS, et al. HDAC6 sustains growth stimulation by prolonging the activation of EGF receptor through the inhibition of rabaptin-5-mediated early endosome fusion in gastric cancer. *Cancer Lett.* 2014;354:97-106.
41. Liang X, Shi H, Yang L, Qiu C, Lin S, Qi Y, et al. Inhibition of polypyrimidine tract-binding protein 3 induces apoptosis and cell cycle arrest, and enhances the cytotoxicity of 5- fluorouracil in gastric cancer cells. *Br J Cancer.* 2017;116:903-911.
42. Beier UH, Wang L, Han R, Akimova T, Liu Y & Hancock WW. Histone deacetylases 6 and 9 and sirtuin-1 control Foxp3+ regulatory T cell function through shared and isoform-specific mechanisms. *Sci Signal.* 2012;5:ra45.
43. Ma GF, Miao Q, Liu YM, Gao H, Lian JJ, Wang YN, et al. High FoxP3 expression in tumour cells predicts better survival in gastric cancer and its role in tumour microenvironment. *Br J Cancer.* 2014;110:1552-60.
44. Suh JH, Won KY, Kim GY, Bae GE, Lim SJ, Sung JY, et al. Expression of tumoral FOXP3 in gastric adenocarcinoma is associated with favorable clinicopathological variables and related with Hippo pathway. *Int J Clin Exp Pathol.* 2015;8:14608-18.
45. Quante M, Bhagat G, Abrams JA, Marache F, Good P, Lee MD, et al. Bile acid and inflammation activate gastric cardia stem cells in a mouse model of Barrett-like metaplasia. *Cancer Cell.* 2012;21:36-51.

Tables

Table 1 Sequence of primers used in the study.

siRNA name	Forward sequence	Reverse sequence
HDAC6	AGTCCATCGCAGATACTGGC	TTAGTCTGGCCTGGAGTGGA
HNF4a	ACATGGACATGGCCGACTACA	AGCTCGCAGAAAGCTGGGAT
FOXP3	GUCUGCACAAGUGCUUUGUTT	ACAAAGCACUUGUGCAGACTT

Table 2 Sequence of primers used in the study.

Primer name	Forward sequence	Reverse sequence
HDAC6	AGTCCATCGCAGATACTGGC	TTAGTCTGGCCTGGAGTGGA
HNF4a	ACATGGACATGGCCGACTACA	AGCTCGCAGAAAGCTGGGAT
FOXP3	CCTACCCACTGCTGGCAAAT	CCTGGCAGTGCTTGAGGAA
HNF4a	(ChIP NC) GAGCCAAGATCGCACCATTGC	GTCATGAGCCACTGTGCCCAAC
	(ChIP 1) AGCTAATTTTTGTATTTTTAG	GCCAAGATCGTGCCACTGCAC
	(ChIP 2) CATATCACTCACCAGTTTGT	CAGGAAGTAGTGGGAAAACCG
	(ChIP 3) ATGGAGACAGCAACAGTCCC	GCCCACCCAGCCGGAGAGCTG
FOXP3	(ChIP NC) GGCTGACATTACCTGCGCCT	TTTCTGGGCCAACAACCACG
	(promoter) AGCACTGTATCTGACCCATGG	CCTGACCCAGCCACTGTCCCAC
	(CNS) CCCGTGATTATCAGCGCACA	GAGCAGGGACACTCACCTTG

Table 3 FOXP3 expression in gastritis and IM tissues.

Histopathological changes	n	FOXP3				p-value
		-	+	++	+++	
Gastritis	24	7	11	4	2	0.0102
IM	80	52	21	6	1	

Table 4 Histopathological changes of gastric mucosa in mice

Histopathological changes (n)	Ctrl/	DCA/	Ctrl/	DCA/	p-value
	WT	WT	Rosa26 ^{Hnf4a}	Rosa26 ^{Hnf4a}	
Normal stomach	8	5	2	0	
Gastritis	0	3	1	3	0.0014
Atrophic gastritis	0	0	4	2	
IM-like lesions	0	0	1	3	

Figures

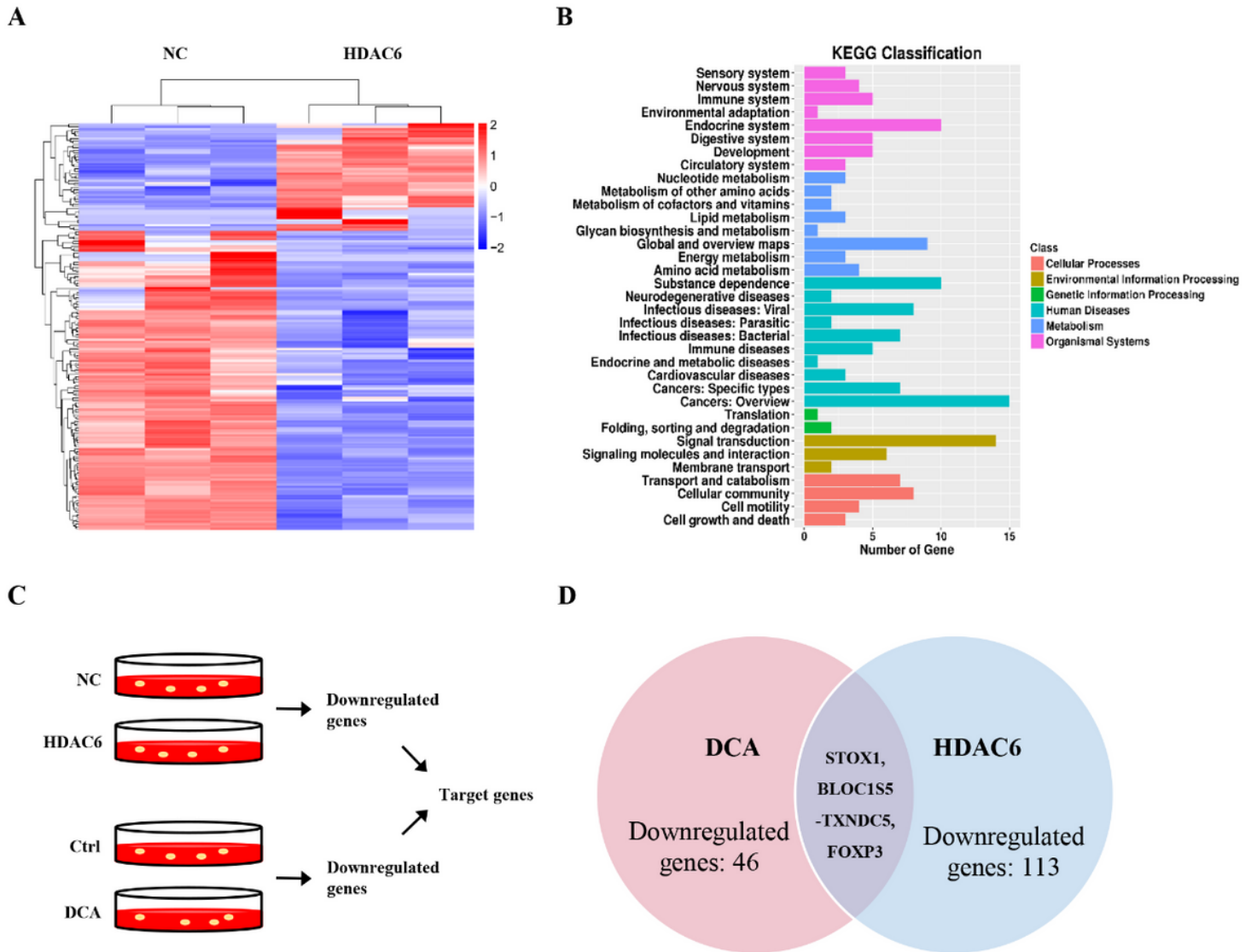


Figure 1

Screening of HDAC6 downstream target genes. a Heatmap of differential messenger RNA (mRNA) expression between negative control (NC) and HDAC6 overexpressed gastric epithelial cell line (GES)-1 cells. Expression values shown are mean values (fold change>2.0; P<0.05). Red: increased expression, blue: decreased expression. b KEGG enrichment analysis of differentially expressed genes. c Workflow to examine the change of genes in GES-1 cells after DCA treatment or HDAC6 overexpression. d The decreased messenger RNA (mRNAs) in mRNA profile of HDAC6 overexpressed cells were overlapped with that of DCA treated GES-1 cells to obtain the predicted potential targets of HDAC6.

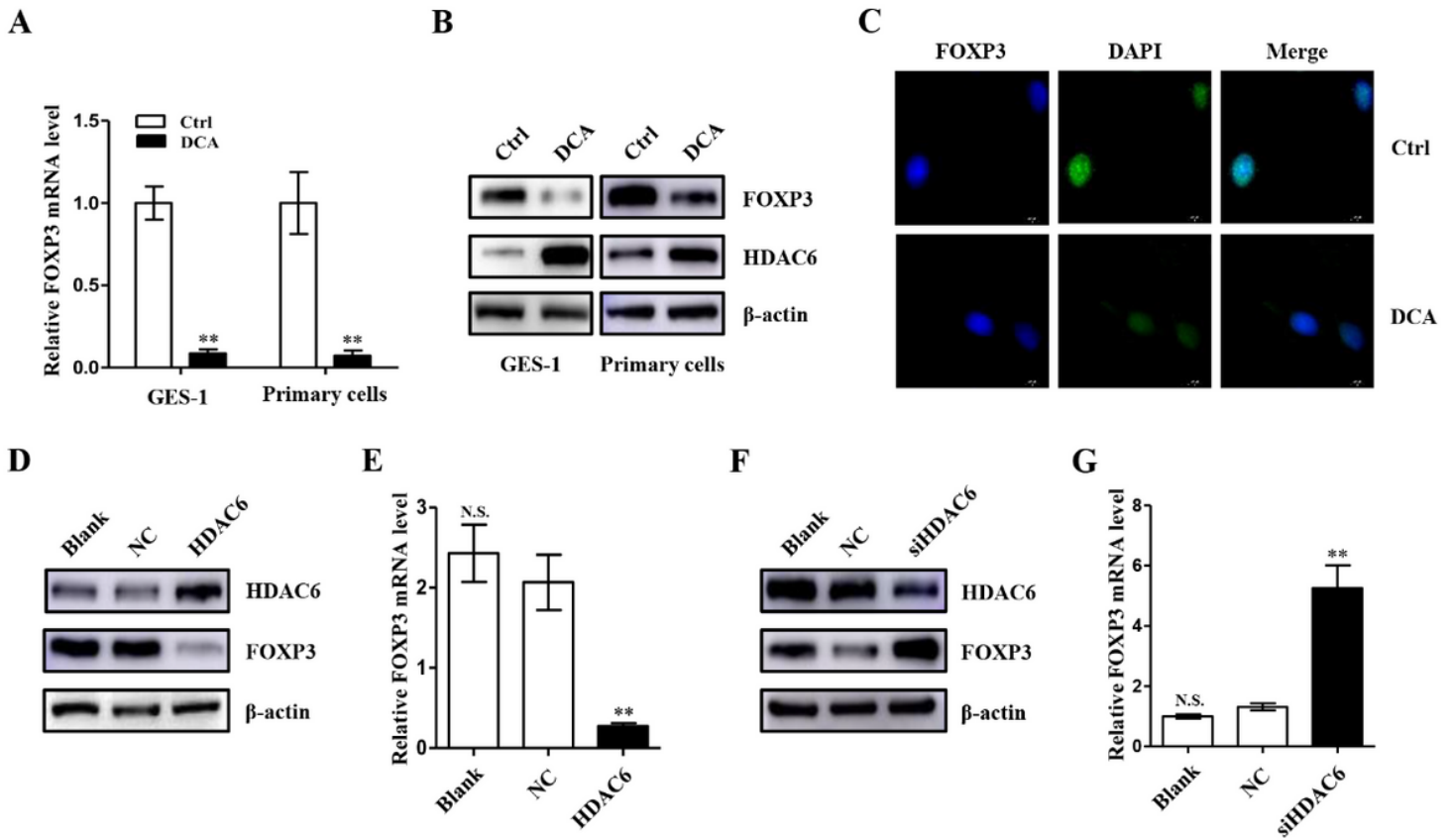


Figure 2

HDAC6 negatively regulates FOXP3 in gastric cells. a mRNA levels of FOXP3 were decreased by DCA treatment in GES-1 cells and primary cells of gastric mucosa in mice. Incubating time: 24 hours; dosage: 100 μ M. β -actin RNA was used as internal control in all qRT-PCR assays. Student's t-test. b Protein levels of FOXP3 and HDAC6 in GES-1 cells and primary cells treated with DCA (100 μ M) for 24 hours. β -actin levels were used as internal control in all immunoblot assays. c Immunofluorescence showed FOXP3 expression in the nuclei of GES-1 cells. d, e Immunoblot and qRT-PCR analysis showed upregulation of HDAC6 by lentiviral vectors led to inhibition of FOXP3. Student's t-test. f, g Knockdown of HDAC6 by small interfering RNA (siRNA) led to increase of FOXP3. Student's t-test. ** $p < 0.01$. N.S., not significant.

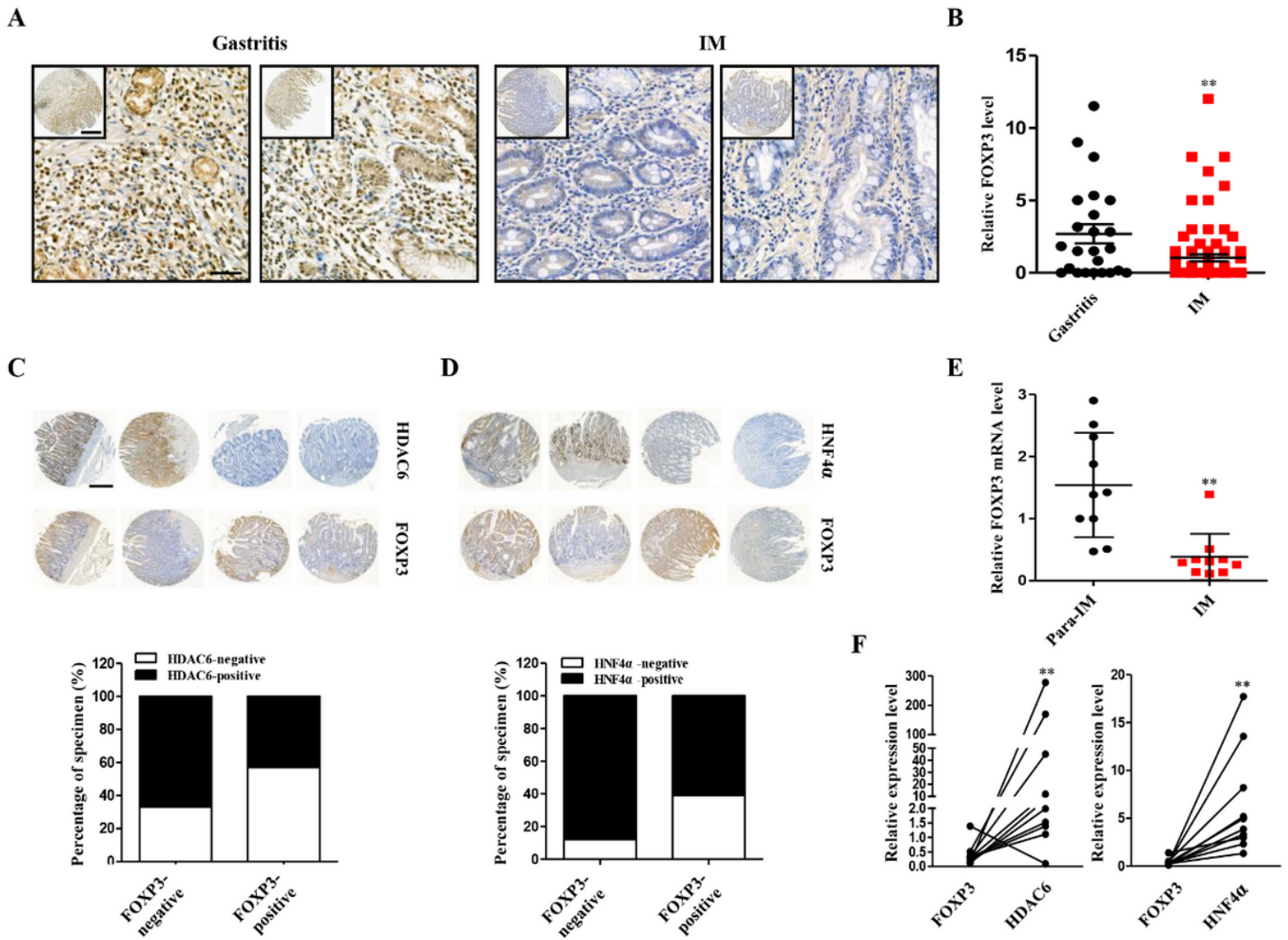


Figure 3

FOXP3 was decreased in gastric intestinal metaplasia (IM). a, b Representative images and analysis of immunohistochemistry (IHC) staining for FOXP3 in gastritis tissues (n=24) and IM tissues (n=80). Student's t-test. Scale bars: 500 μ m (top); 50 μ m (bottom). c, d IHC staining for FOXP3, HDAC6 and HNF4a in serial sections of IM tissues and the association between FOXP3, HDAC6 (left) and HNF4a (right) expression levels in these specimens. Student's t-test. Scale bar: 500 μ m. e qRT-PCR results of expression of FOXP3 in 10 paired IM and surrounding tissues. f Comparison of FOXP3, HDAC6 and HNF4a mRNA expression in the biopsies. ** $p < 0.01$.

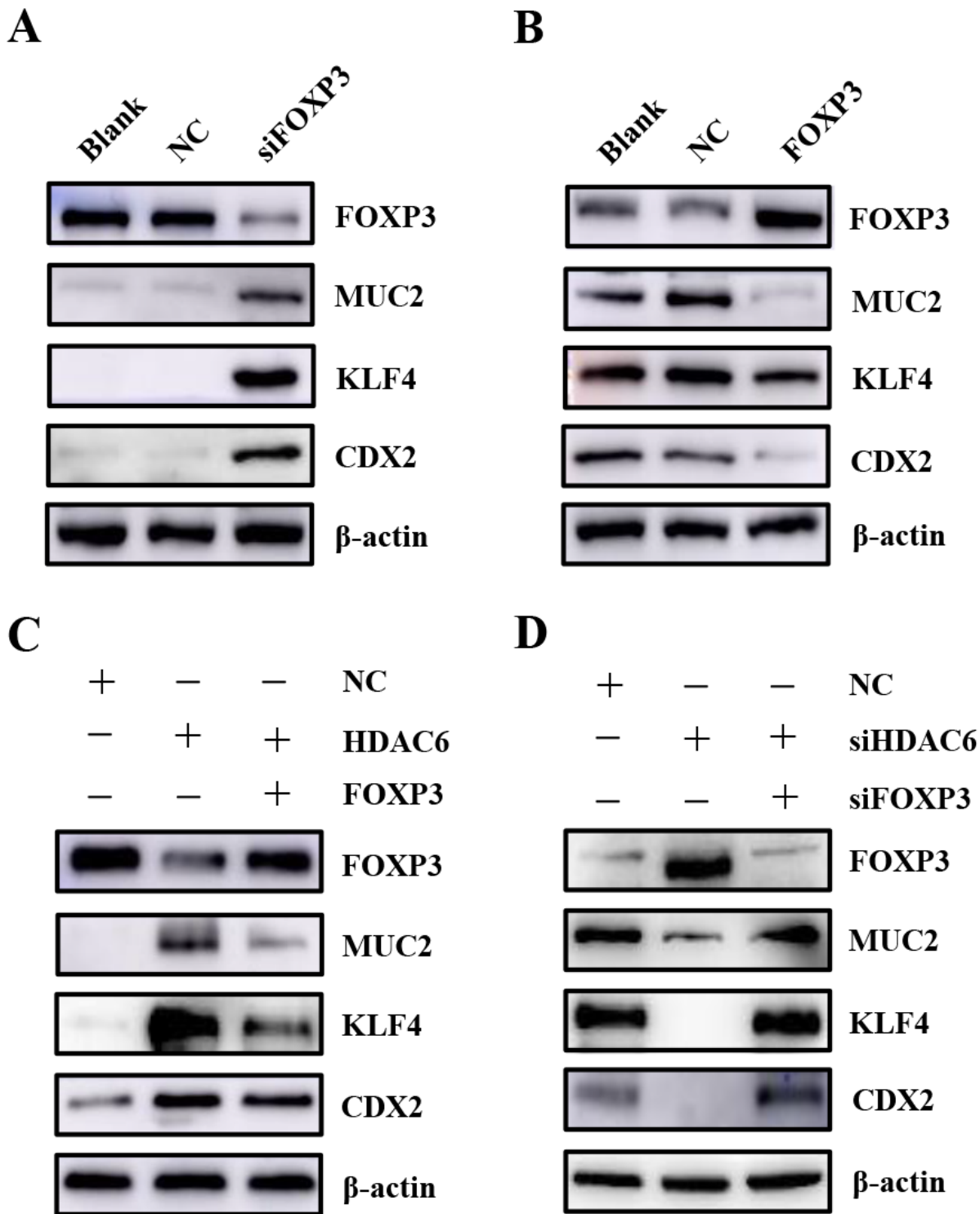


Figure 4

FOXP3 inhibited the expression of intestinal markers in gastric cells. a Downregulation of FOXP3 caused consequential enhancement of MUC2, KLF4 and CDX2 in GES-1 cells. b Intestinal markers were decreased by FOXP3 overexpression in AGS cells. c The enhancement of intestinal markers induced by HDAC6 overexpression was diminished by upregulation of FOXP3 in GES-1 cells. d Knockdown of FOXP3 rescued expression of intestinal markers reduced by siHDAC6 in AGS cells. ** $p < 0.01$. N.S., not significant.

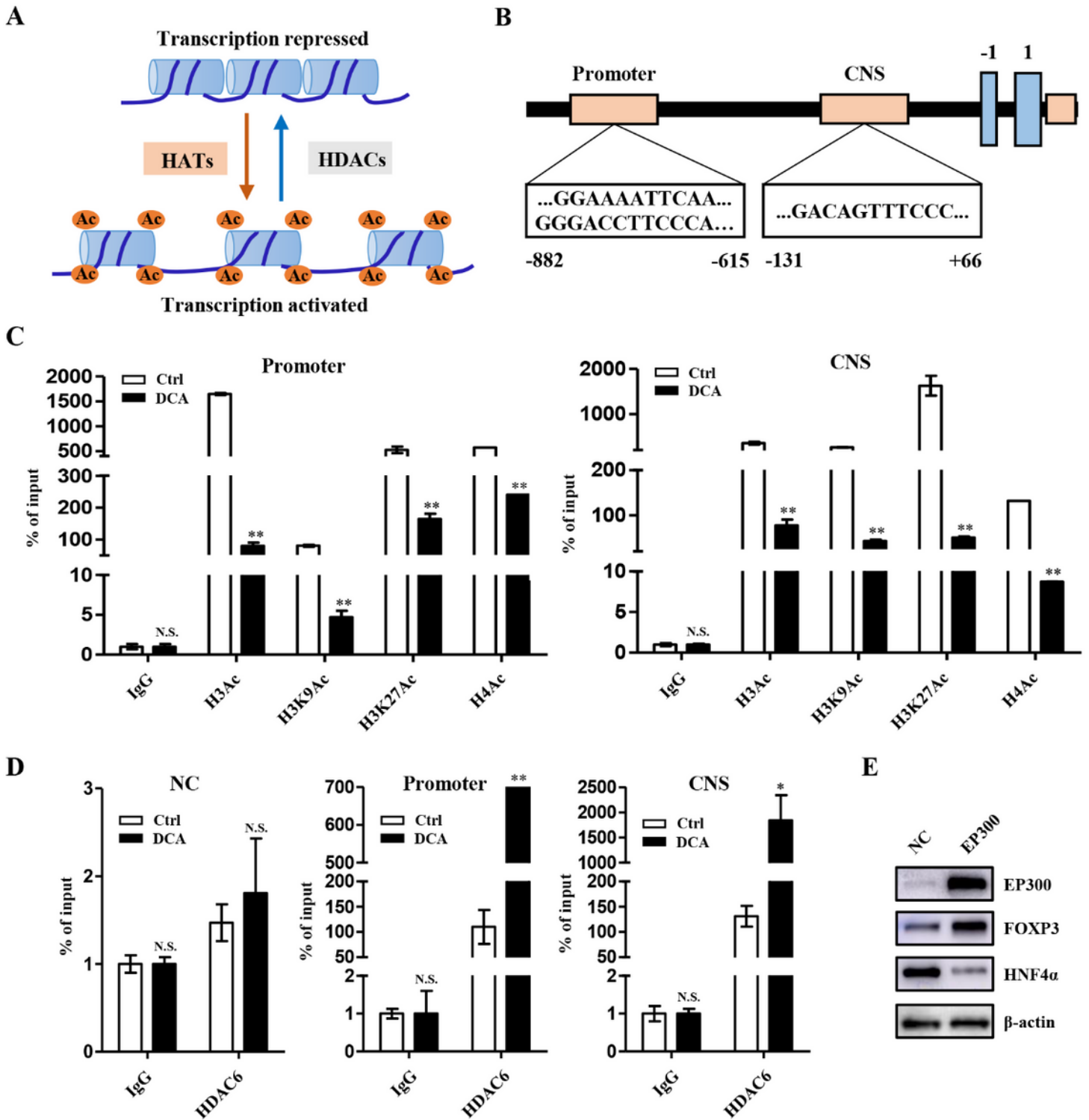


Figure 5

HDAC6 induces extensive chromatin modifications at FOXP3 loci. a Histone acetyltransferase (HATs) and histone deacetylases (HDACs) affect the dynamics of chromatin remodeling during gene transcription. b Schematic diagram depicting FOXP3 locus structure and the sequences in the FOXP3 promoter and CNS regions. c ChIP assays for H3Ac, H3K9Ac, H3K27Ac, H4Ac modifications in FOXP3 locus. IgG serves as immunoprecipitation control. Student's t-test. d ChIP assays for HDAC6 in FOXP3 promoter and CNS

regions in GES-1 cells. Student's t-test. e FOXP3 and HNF4 α protein levels was examined by western blot analysis in AGS cells treated with EP300-expressing vectors or control. * $p < 0.05$, ** $p < 0.01$. N.S., not significant.

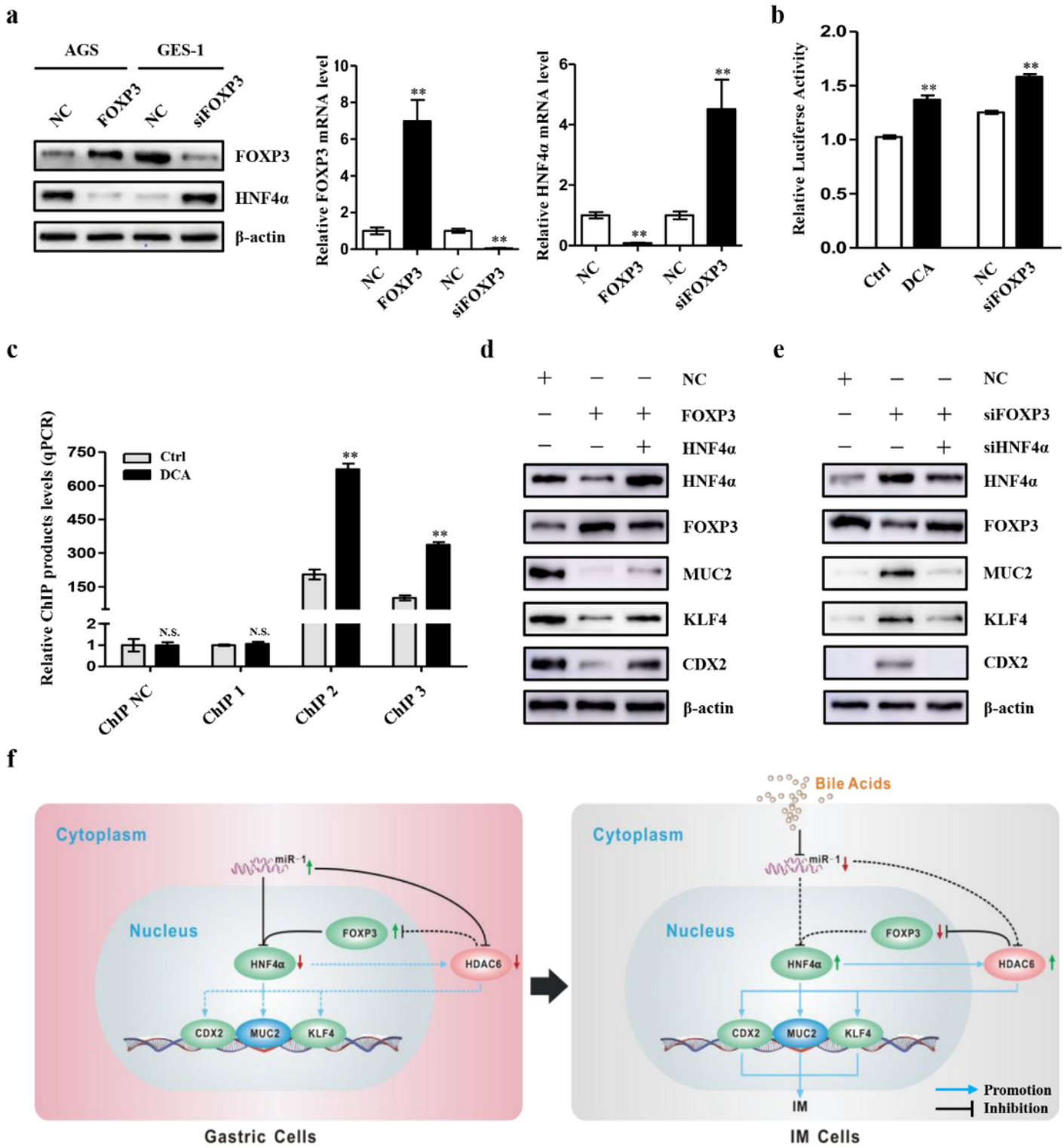
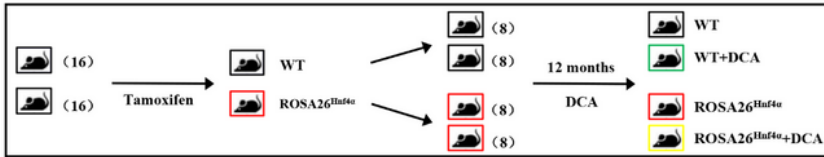


Figure 6

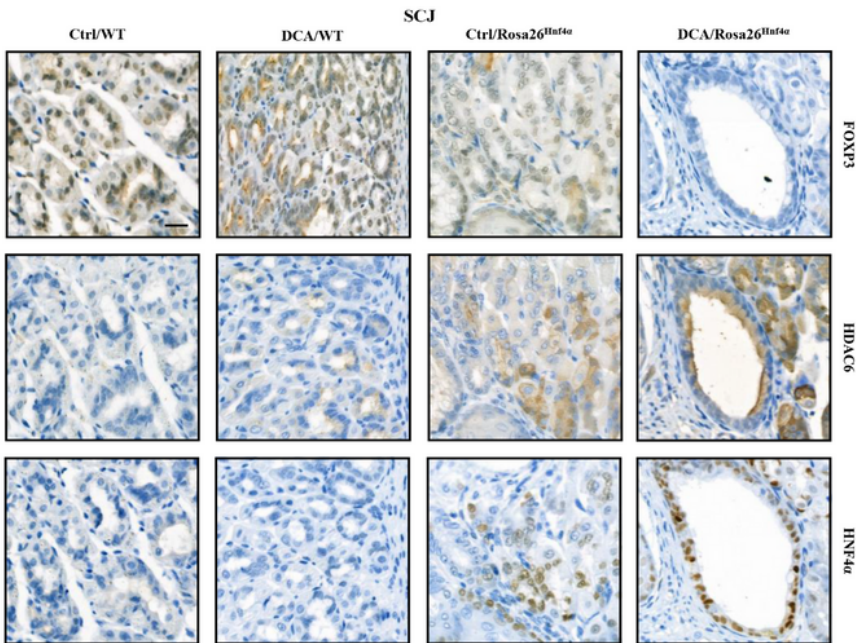
FOXP3 negatively regulated HNF4 α transcription. a FOXP3 inversely regulated HNF4 α at both mRNA and protein levels. Student's t-test. b The promoter activity of HNF4 α was enhanced by DCA and siFOXP3

treatment in GES-1 cells. Student's t-test. c A CHIP assay demonstrated the direct binding of FOXP3 to the HNF4 α promoter in GES-1 cells. Student's t-test. d AGS cells were co-infected with FOXP3-expressing vectors and HNF4 α -expressing vectors. The expression of intestinal markers was detected by immunoblot. e Upregulated intestinal markers expression induced by siFOXP3 was attenuated by siHNF4 α in GES-1 cells. f A schematic model of miR-1/HDAC6/FOXP3/HNF4 α pathway in gastric cells. In response to BA, miR-1 inhibition promotes HNF4 α and HDAC6, which increase the transcription of intestinal markers including MUC2, KLF4 and CDX2. ** $p < 0.01$. N.S., not significant.

A



B



C

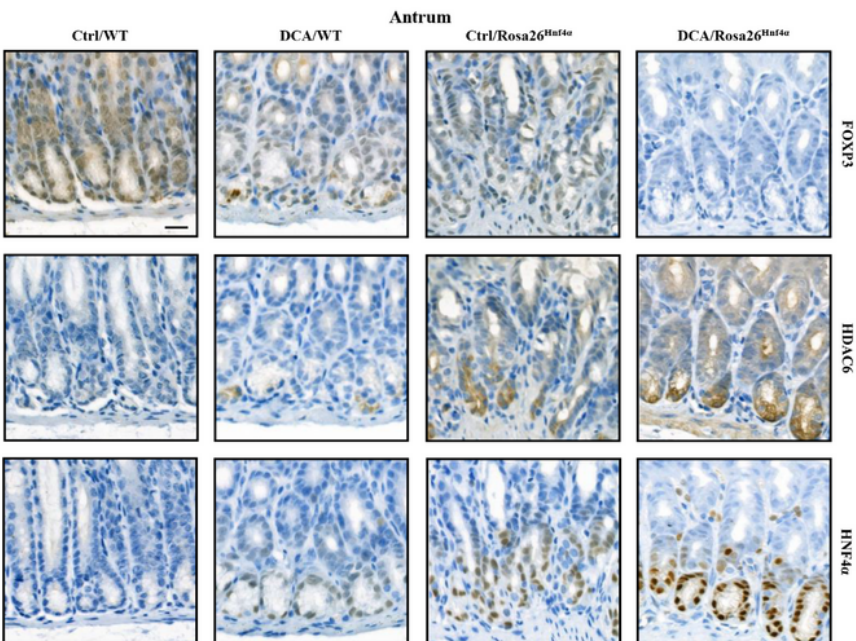


Figure 7

HDAC6/FOXP3/HNF4 α loop in mice. a Experimental strategy of establishing gastric intestinal metaplasia model in mice. Active Hnf4 α expression was induced after tamoxifen treatment. b Representative pictures of IHC staining for FOXP3, HDAC6 and HNF4 α at the SCJ of WT and Rosa26Hnf4 α mice with or without DCA treatment. Scale bars: 100 μ m (top); 20 μ m (bottom). c Expression of these molecules in the gastric antrum of four groups of mice. Scale bars: 100 μ m (top); 20 μ m (bottom).

Supplementary Files

This is a list of supplementary files associated with this preprint. Click to download.

- [Additionalfile1.pdf](#)